www.czasopisma.pan.pl PAN www.journals.pan.pl

ARCHIVES of FOUNDRY ENGINEERING

ISSN (2299-2944)

10.24425/afe.2024.151316

Published quarterly as the organ of the Foundry Commission of the Polish Academy of Sciences

Structure of ADI Cast Iron as a Cast *"in situ"* Composite Reinforced with TiC Ceramic Particles

J. Marosz *, M. Kawalec, M. Górny
AGH University of Krakow, Poland
* Corresponding author: E-mail address: marosz@agh.edu.pl

Received 22.07.2024; accepted in revised form 01.10.2024; available online 24.12.2024

Abstract

This paper presents a novel technology for the production of a casting material, which is an "in situ" composite on an ADI iron matrix reinforced with titanium carbide particles. As a result of the initiated Self-propagating High-temperature Synethesis reaction in Bath (liquid metal) of the type "solid Ti" – "solid C" type, led to the formation of ceramic phases in the form of titanium carbides. This method, allowed the synthesis of a cast composite based on ductile cast iron and, after subsequent heat treatment, the transformation of this material into ADI cast iron. The greatest advantage of "in situ" composites is that they are produced in a one-step metallurgical process, which is characterised, among other things, by: high thermodynamic stability, synthesis of a reinforcing phase in a metal bath, small size of ceramic particles with the possibility of controlling their dimensions by reaction kinetics parameters during the synthesis process. In this study, metallographic analysis of the composite obtained, both in the initial state and after heat treatment, was carried out using optical and scanning electron microscopy. An analysis of the chemical composition in the micro-area was carried out using the EDS method, the chemical composition was studied using the XRF spark X-ray fluorescence method, and the proportion of graphite and the carbide phase, i.e. titanium carbide TiC, was determined. The results obtained confirmed the possibility of obtaining the composite material via the SHSB reaction route. The heat treatment results showed that the carbides are thermodynamically stable and do not dissolve at temperatures designed for the production of ADI cast iron. The SHSB reaction guarantees a uniform distribution of titanium carbides on the ADI cast iron matrix.

Key words: ADI cast iron, „in situ" composites, SHSB reaction, MMCs composites, titanium carbide TiC, microstructures, heat treatment.

Nomenclature:

- ***FGI*** *– flake cast iron with TiC particles,*
- ***SGI*** *– ductile cast iron with TiC particles,*
- ***a*** *– heat treatment conzisting of austenitizing at 900°C for 120 min, holding in salt bath at 380°C for 60 min,*
- ***b*** *– heat treatment conzisting of austenitizing at 900°C for 120 min, holding in salt bath at 380°C for 240 min,*
- ***FGIa*** *– flake cast iron with TiC particles, after a type of heat treatment,*
- ***SGIa*** *– ductile cast iron with TiC particles, after a type of heat treatment,*
- ***FGIb –*** *flake cast iron with TiC particles, after b type of heat treatment,*
- ***SGIb*** *– ductile cast iron with TiC particles, after b type of heat treatment,*
- ***ADI*** *– Austempered Ductile Cast Iron,*
- ***SHS*** *– Self propaging High-temperature Syntesis,*
- ***SHSB*** *– Self propaging High-temperature Syntesis in Bath,*
- ***MMCs*** *– Metal Matrix Composites,*
- ***ROM*** – Rule of Mictures.

1. Introduction

ADI cast iron is characterised by very favourable service properties, combining high ductility and material strength. ADI cast iron owes its good ductility to the spheroidal graphite separations and its high strength to the ausferritic matrix [1-7]. These properties of ADI cast iron predispose it to a wide range of applications, including automotive, construction, railways, agriculture, in the construction of all kinds of brackets, gears, crankshafts, etc. [8]. ADI cast iron charakterised by relatively low manufacturing cost compared to many steels or cast steel grades, while maintaining very good performance properties. It exhibits approximately twice the tensile strength of typical ductile cast iron, similar to ductile and heat-treated steel, with improved ductility properties, good fatigue resistance and wear resistance. It has a favourable thermal conductivity coefficient and vibration damping ability, making it a more versatile material compared to some steels, while being more cost-effective to produce [3, 4].

Each engineering material such as cast steel or cast iron (including ausferritic matrix cast iron e.g. ADI, VAGI, SiSSADI, etc.), has certain limitations. These materials have at some point reached the maximum of their functional and mechanical capabilities. The transformation of ADI cast iron into a composite material, according to the ROM mixture principle valid for composite materials, opens up new possibilities for its applications. Since it is enriched with a ceramic phase such as TiC, ADI cast iron becomes a completely new material [9, 10].

The high-temperature synthesis reaction in a metal bath (SHSB), makes it possible to obtain a wide group of compounds, i.e.: carbides, borides and nitrides [11, 12]. This article presents the synthesis process for titanium carbides, selected for their very favourable enthalpy of formation and attractive functional properties such as high hardness and melting point, and high thermodynamic stability [9, 10, 13]. The SHSB reaction guarantees that a ceramic phase, which is a solid when the matrix is still a liquid phase, is obtained already at the metal bath stage. The ceramic phase formed in this way is thermodynamically stable, so that when the heat treatment required to obtain an ausferritic matrix is carried out, its presence does not interfere with this process. The SHSB reaction, due to its versatility, offers the possibility of transforming any (metal) material into a cast composite material [11, 12]. In works [13, 14], the functional properties of “in situ” composite materials of the MMCs type were presented, including increased strength, increased stiffness, increased resistance to abrasive wear, improved mechanical properties, dimensional stability at elevated temperatures and a favourable density-to-performance ratio.

Titanium, is one of the elements adversely affecting the spheroidisation process due to its deformation of spheroidal graphite [14-16]. In the study, it was observed and confirmed that titanium, which was present in semi-finished products (powder mouldings containing compressed titanium and carbon powders) after SHSB synthesis, affected the character of the morphology of graphite precipitates by deforming them.

There is a lack of information in the national and world literature about attempts to transform ADI cast iron via a high-temperature synthesis reaction in a metal bath (SHSB) into a cast “in situ” composite of the MMCs type. The aim of this study is to fill this gap and to present the results of basic research.

2. Experimental procedures

2.1. Fabrication of ductile cast iron enriched in titanium carbides TiC

In order to obtain cast iron with a perlitic matrix and a near-perlitectic composition, the following input materials were used: casting pig iron Sorelmetal (8.3 kg), steel scrap (1.47 kg), nickel (0.105 kg), Si-tech. (0.07 kg), Fe-Mn (0.045 kg) and Fe-S (0.002 kg). Smelting was carried out in a medium-frequency induction furnace (8 kHz).

A key element of the experiment was the preparation of Ti and C powder briquettes, which produced a composite material: ductile iron/TiC by SHSB reaction. The briquettes contained titanium and graphite powders with a granulation of 4 μm in an atomic ratio of 55% Ti and 45% C. The weighted blends prepared in this way were subjected to air-free 3D mixing for a period of 2 hours to homogenise the mixture throughout. Subsequently, the compositions of titanium and carbon powders were compressed and constituted intermediates for SHSB synthesis introduced into the metal bath (using the bell method). The mass of the briquettes introduced into the liquid metal was 0.5 kg to ensure that the proportion of the ceramic phase in the resulting composite was up to 5%.

The spheroidisation process used an iron-silicon-based spheroidiser with a magnesium content of 5.5 per cent in an amount of 0.2kg to the charge weight, and an iron-silicon-based modifier with a nickel content of 0.75 per cent in an amount of 0.07kg to the charge weight.

The molds used in the experiment were wedge-shaped with a constant wall thickness of 25mm. Additionally, a chill mold in the shape of a disc was prepared, which was designated for chemical composition analysis using the XRF method.

The smelting consisted of the following steps:

- melting of the raw materials and superheating of the alloy to 1490°C,
- transfer of the crucible to the spheroidisation furnace and introduction of the briquettes into the crucible with the liquid metal (formation of the ceramic phase by SHSB reaction)
- transfer the crucible to the furnace, followed by reheating to 1490°C and ensuring, by means of eddy currents in the induction furnace, distribution of the TiC carbides in the entire metal volume,
- transfer the crucible to the spheroidisation post and carry out the spheroidisation treatment with modification by bell method,
- transfer the crucible again to the furnace for about one minute to calm the metal bath before pouring into the moulds,
- pour the moulds.

2.2. Heat treatment

The heat treatment used included an austenitisation process in a Czylok FCF 22H heat treatment chamber furnace and an iznothermic transformation quenching process in a salt bath

furnace ($NaNO_2$ - KNO_3). The heat treatment was performed in two variants: a and b (heat treatment parameters are shown in table 1).

Table 1.
Applied heat treatment parameters

Type of heat trearment	Temperature of austenitisation, T_γ, °C	Time of austenitisation, τ_γ, min	Quenching temperature with isothermal transformation, T_{pi}, °C	Hardening time with isothermal transition, τ_{pi}, min
a	900	120	380	60
b	900	120	380	240

2.3. Examination of chemical composition

The chemical composition of the composite samples obtained was studied by spark X-ray fluorescence (XRF) using a SPECTRO MIDEX spectroscope. Six measurements were taken on each sample, from which the average value was determined.

2.4. Structural research

Metallographic specimens were made using Metkon® FORCIPOL® 1V GRINDER - POLISHER apparatus, where, after the specimens were incrusted, they were ground on grinding wheels with gradations: 120, 220, 500, 600, 1200 and 2000 µm, and then polished on a polishing cloth in diamond slurries with gradations: 9, 3 and 1µm. The metallographic deposits were etched with Nital reagent (5% nitric acid (V) + 95% ethanol). Photographs of the microstructures and measurements of the surface contribution of the reinforcing phase particles (TiC carbides) were taken, using a KEYENCE VHX - 7000 DIGITAL MICROSCOPE.

Measurements were made according to the following methodology: on the basis of ten randomly selected areas at 500x magnification, the ratio of the area occupied by the TiC phase to the total area examined was determined.

The surface area ratio for graphite precipitates, was measured using a LEICA MEF 4-M optical microscope and dedicated Leica QWin software. The measurement methodology was as follows: based on a random selection of ten locations on the surface of the microstructure, the ratio of the area of the graphite precipitates to the total area measured was determined at a magnification of 200x. In addition to the surface area ratio of graphite, the graphite shape factor W_k and the equivalent diameter of the graphite precipitates were also determined using this op- portation. The W_k index was calculated using the formula (1):

$$W_k = \frac{4\pi A}{p^2} \quad (1)$$

where:
A - surface area of graphite particles (µm^2),
p - circumference of graphite particles (µm).

2.5. Scanning electron mikroskopy

A scanning electron microscope study was also carried out to visualise the morphology of the graphite precipitates and titanium carbides that formed in the metal matrix during the SHSB synthesis reaction. The EDS method was used to analyse the chemical composition in the micro-area of the microstructure components for identification and verification. The study was performed using a Jeol JSM 5500LV scanning microscope with a resolution of 4nm, equipped with an EDS (energy dispersive spectrometry) system from IXRF (USA) for X-ray microanalysis.

3. Results

3.1. Chemical composition results (XRF)

Table 2 shows the results of the chemical composition of the composite materials obtained. The increased titanium content is due to the presence of this element in the briquettes and the course of the SHSB reaction.

Table 2.
Chemical composition obtained by XRF method

Type of sample	Chemical composition, % wt.								
	C	Si	Mn	P	S	Mg	Ni	Ti	Fe
FGI	*3.65*	*1.28*	*0.43*	*0.07*	*0.03*	*0.00*	*1.08*	*0.97*	*Bal.*
SGI	*3.48*	*2.44*	*0.44*	*0.06*	*0.01*	*0.03*	*1.04*	*0.80*	*Bal.*

FGI – flake cast iron with TiC particles form SHSB reaction,
SGI – nodular cast iron with TiC particles after SHSB reaction.

The decrease in carbon content in the composite material after the ductoidisation treatment may be due to the long holding time of the metal bath at high temperature in order to homogenise the TiC ceramic particles throughout. A magnesium content that is too low, as for ductile cast iron, may be due to a too high scaling of this element during the spheroidisation process.

3.2. Metallographic analysis

Figure 1 shows images of the microstructures of the obtained FGI and SGI composite materials in the etched and unetched states. From metalografic analysis, it can be seen that the synthesis of titanium carbides in the iron was successful and a composite material was obtained. The microstructure of the FGI composite shows uniformly distributed titanium carbide precipitates, flake graphite characteristic of grey cast iron, and a perlitic matrix that contains cementite eutectic precipitates.

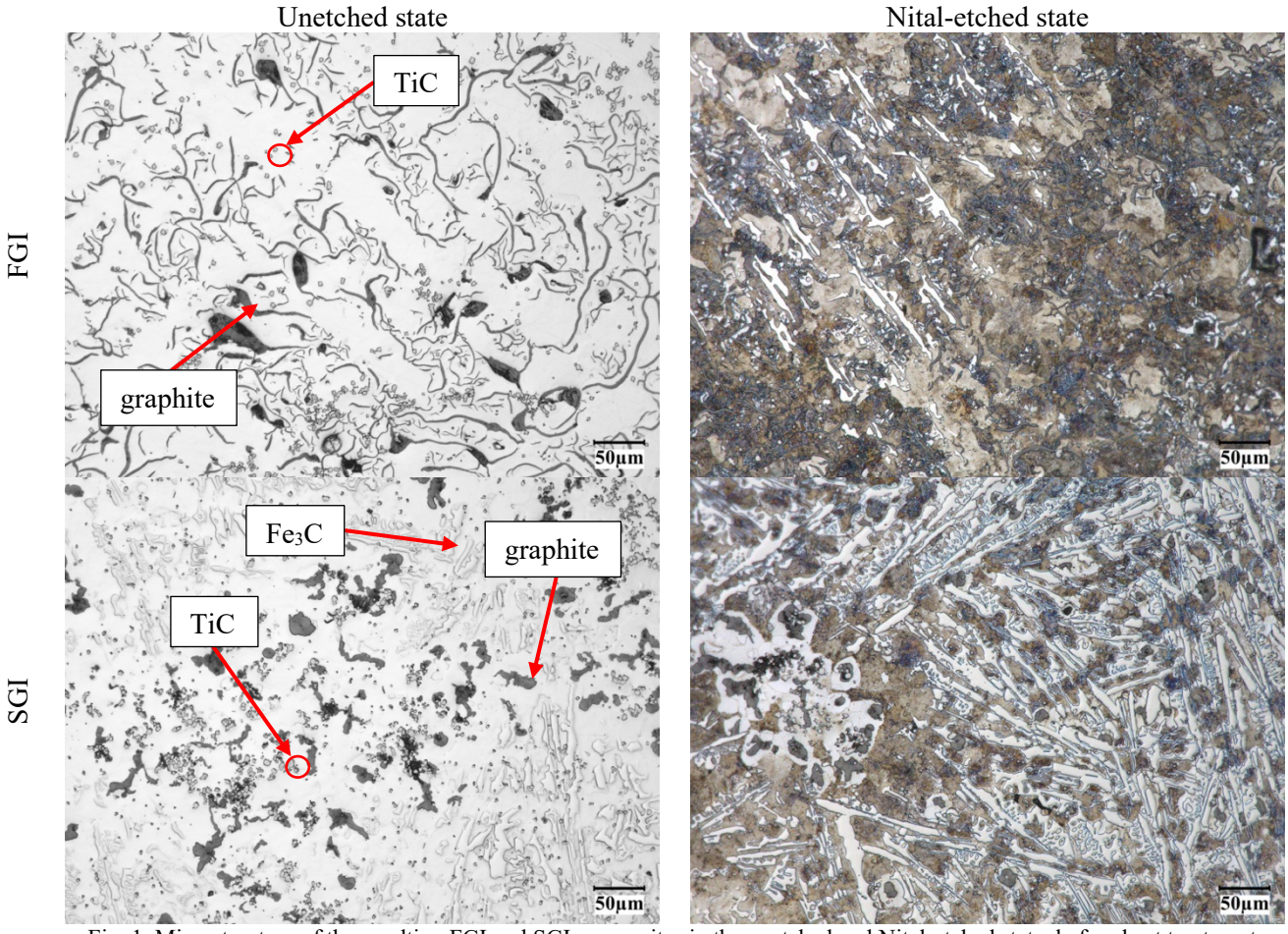

Fig. 1. Microstructure of the resulting FGI and SGI composites in the unetched and Nital-etched state, before heat treatment, 500x

In the microstructure of the SGI composite, the influence of the spheroidisation process is visible, which caused a change in the shape of the graphite. Due to the too low magnesium content, a typical vermicular graphite shape was obtained. A high proportion of cementitic eutectics was also observed in the resulting composite material. The increase in the proportion of cementitic eutectics in the composite after the spheroidisation treatment may be due to the kinetics of the SHSB reaction and the reduction in carbon content. The structure of the SGI composite conteins of: vermicular graphite particles, titanium carbides, a perlitic-ferritic matrix with numerous cementitic eutectic precipitates. In the case of composite SGI, part of the titanium carbides is evenly distributed, while part tends to cluster near the vermicular graphite.

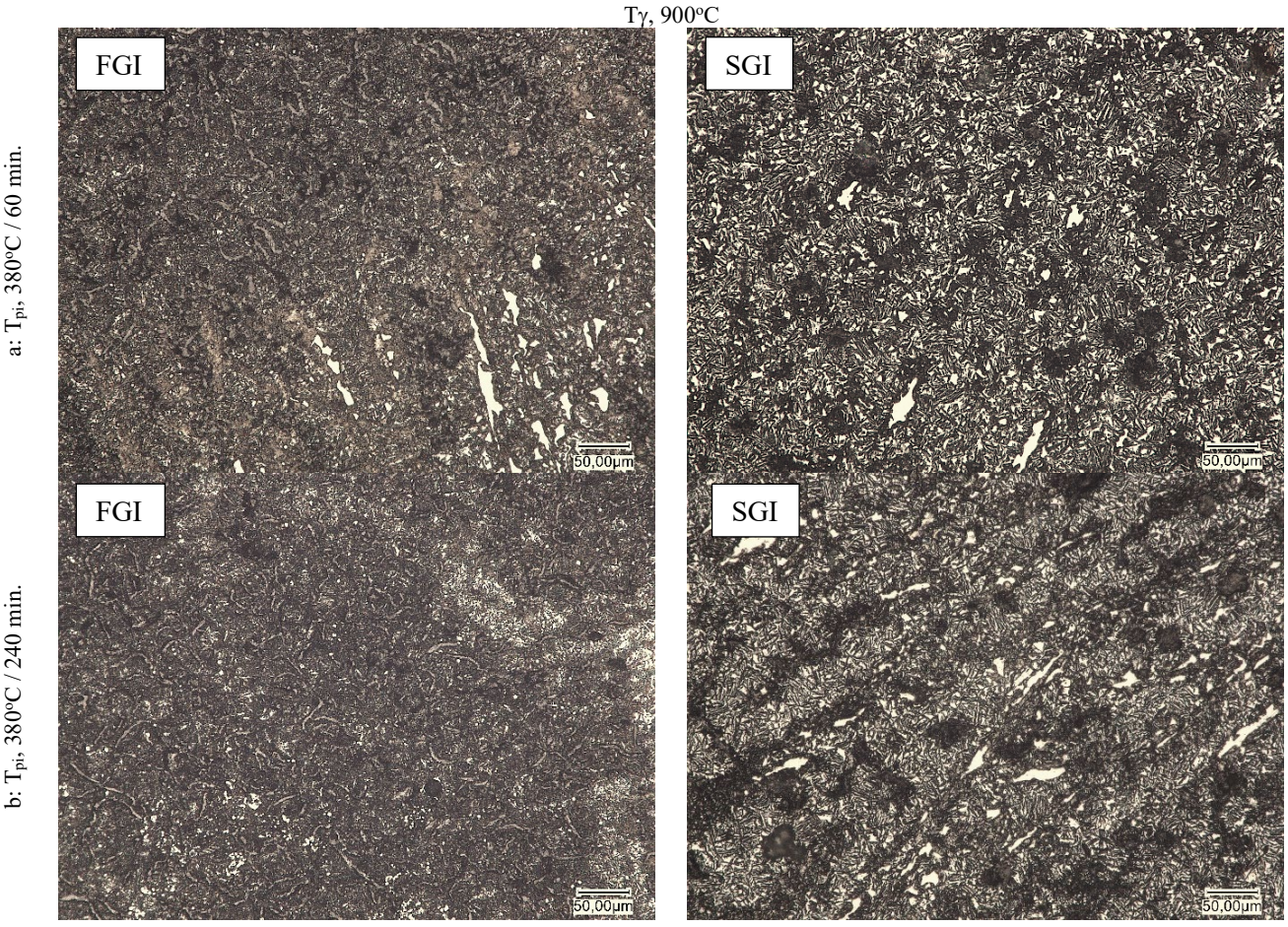

Fig. 2. Microstructure of FGI and SGI composites after heat treatment in two variants a and b, austenitisation temperature (T_γ), austepering temperature (T_{pi}), 500x, Nital etched.

Fig. 2 shows images of the microstructures of the composite materials obtained, after heat treatment, in the etched and un-etched state The microstructure analysis shows that an ausferritic matrix was obtained. The carbides obtained by the SHSB method, being thermodynamically stable, do not interfere with this process. The application of the heat treatment, in addition to changing the matrix, led to the elimination of the presence of cementitic eutectics to a large extent, but did not remove it completely.

Table 3.
Structural test results

Type of sample	S_f	VI, %	V, %	IV, %	A_{gr}, %	A_{TiC}, %	N_{gr}, µm^{-2}	W_k, -	d_{ekw}, µm
FGI	-	-	-	-	*9.16*	*~4.00*	*7620.18*	*0.29*	-
SGI	*35.00*	*2.60*	*12.40*	*85.00*	*7.26*	*~4.00*	*473.55*	*0.58*	*18.09*
FGIa	-	-	-	-	*12.73*	*~4.00*	*8913.29*	*0.28*	-
SGIa	*37.94*	*5.44*	*32.48*	*63.14*	*8.38*	*~4.00*	*823.88*	*0.59*	*18.08*
FGIb	-	-	-	-	*12.98*	*~4.00*	*8905.24*	*0.25*	-
SGIb	*38.9*	*1.1*	*37.8*	*61.1*	*8.90*	*~4.00*	*850.45*	*0.51*	*18.22*

S_f – degree of spheroidality for graphite separations according to the standard ISO 945-4:2019,
VI, V, IV – distribution by shape of the graphite separations according to the standard ISO 945-4:2019, %,
A_{gr} – surface area share of graphite, %,
A_{TiC} – surface area share of titanium carbides, %,
N_{gr} – number of graphite separations per unit area, µm^{-2},
W_k – shape factor of graphite (determined from equation 1),
d_{ekw} – equivalent diameter of graphite, µm.

Table 3 shows the results of metallographic parameters for FGI and SGI alloys before and after heat treatment (carried out in two variants). For composite SGI, the aspect ratio was 0.58, indicating that it is vermicular graphite. This is also confirmed by literature data [14]. The measured degree of ductility for composite SGI is 35, which is too low for ductile iron. In addition to the degree of ductility, the distribution of graphite particles by shape, according to ISO 945-4:2019, was included. This classification showed that the proportion of graphite most close to perfectly spherical is at 3% (type VI) and the proportion of graphite most degraded at 70% (type IV).

The graphite fraction for composite SGI was 7.26%, for SGIa 8.36% and for SGIb 8.90%, while the equivalent diameter in each case is about 18 µm. The surface share of graphite for the W composite was 9.16%, for FGIa 12.73% and for FGIb 12.98. The value of the aspect ratio for FGI, FGIa and FGIb composites is similar and is approx. 0.3, while for SGI, SGIa and SGIb composites they are in the range 0.51 - 0.59. The proportion of graphite increased after both heat treatment variants, due to dissolution of the cementitic eutectic and secondary graphite particles.

The share of surface titanium carbide for both SGI and FGI comoposite materials was about 4%, while the assumed share was expected to be about 5%. Some of the titanium from the briquette, which was not consumed during the SHSB reaction to form TiC carbides, passed into solution by diffusion and some into the slag, due to titanium's strong affinity for oxygen.

3.3. Scanning electron mikroskopy results

Figures 3-5 show microstructures made using scanning electron micrographs and spectra corresponding to the analysis of titanium carbides, while tables 4-6 show the results of the chemical composition analysis of the individual microstructure components by EDS.

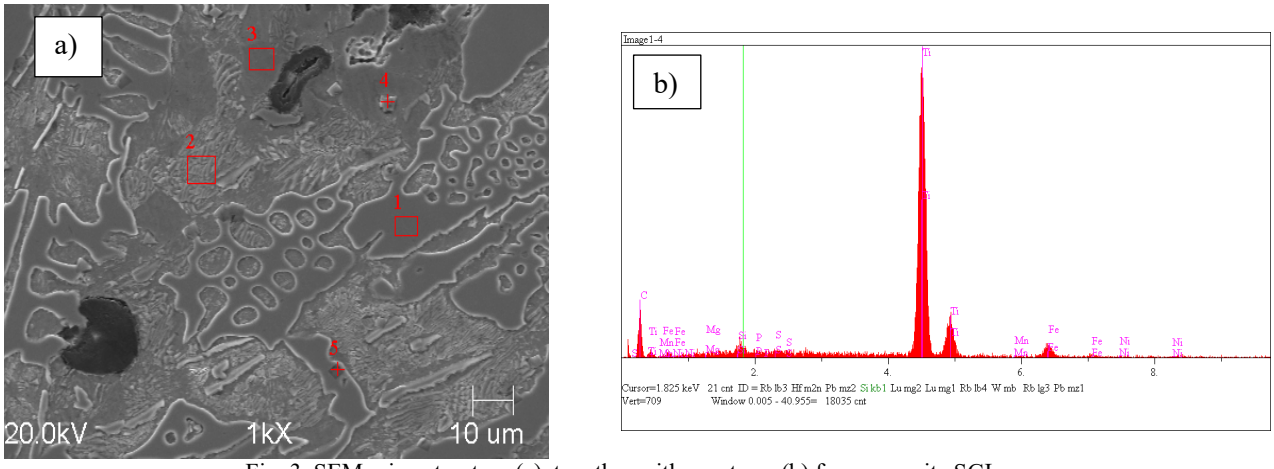

Fig. 3. SEM microstructure (a), together with spectrum (b) for composite SGI

Table 4.
EDS chemical composition results for the composite SGI

Spot	Chemical composition, % wt.								
	C	Si	Mn	P	S	Mg	Ni	Ti	Fe
1	*7.492*	*0.122*	*0.151*	*0.173*	*0.125*	*0.058*	*0.388*	*0.104*	*Bal.*
2	*8.763*	*2.560*	*0.178*	*0.083*	*0.155*	*0.123*	*0.953*	*0.127*	*Bal.*
3	*1.825*	*3.818*	*0.183*	*0.009*	*0.052*	*0.258*	*1.731*	*0.110*	*Bal.*
4	*30.977*	*0.754*	*0.000*	*0.190*	*0.205*	*0.073*	*0.226*	*62.580*	*Bal.*
5	*19.627*	*0.781*	*0.120*	*0.053*	*0.114*	*0.040*	*0.089*	*49.684*	*Bal.*

EDS analysis shows that the carbides obtained are typically TiC wall titanium carbides, obtained by the SHSB reaction route (fig. 3). The EDS chemical composition results (table 4) showed an increased titanium content in the matrix.

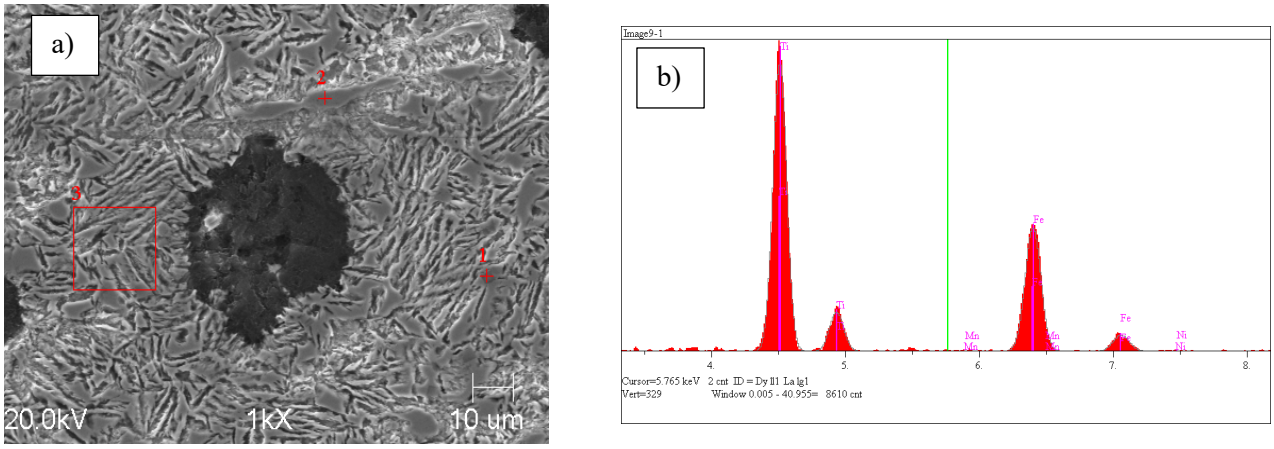

Fig. 4. SEM microstructure (a) and spectrum (b) for the SGIa composite

Table 5.
EDS chemical composition results for SGIa composite

Spot	Chemical composition, % wt.								
	C	Si	Mn	P	S	Mg	Ni	Ti	Fe
1	*21.101*	*0.992*	*0.167*	*0.099*	*0.281*	*0.055*	*0.280*	*40.198*	*Bal.*
2	*16.631*	*0.184*	*0.134*	*0.037*	*0.044*	*0.249*	*0.444*	*0.248*	*Bal.*
3	*11.010*	*2.066*	*0.227*	*0.115*	*0.112*	*0.075*	*0.643*	*1.477*	*Bal.*

Fig. 4 shows the obtained microstructure of the SGIa composite, consisting of an ausferritic matrix with visible separations of cementitic eutectics, graphite in bead form and titanium carbides obtained from the SHSB reaction. SEM microstructure analysis confirms that ausferritic matrix, titanium carbides and cheals have been obtained, the proportion of which has been altered by heat treatment. Also noticeable is the occurrence of block austenite in the microstructure of the SGIa composite, which. formed as a result of choosing too high an austenitisation temperature, i.e. annealing the sample in a furnace in order to homogenise it throughout its volume.

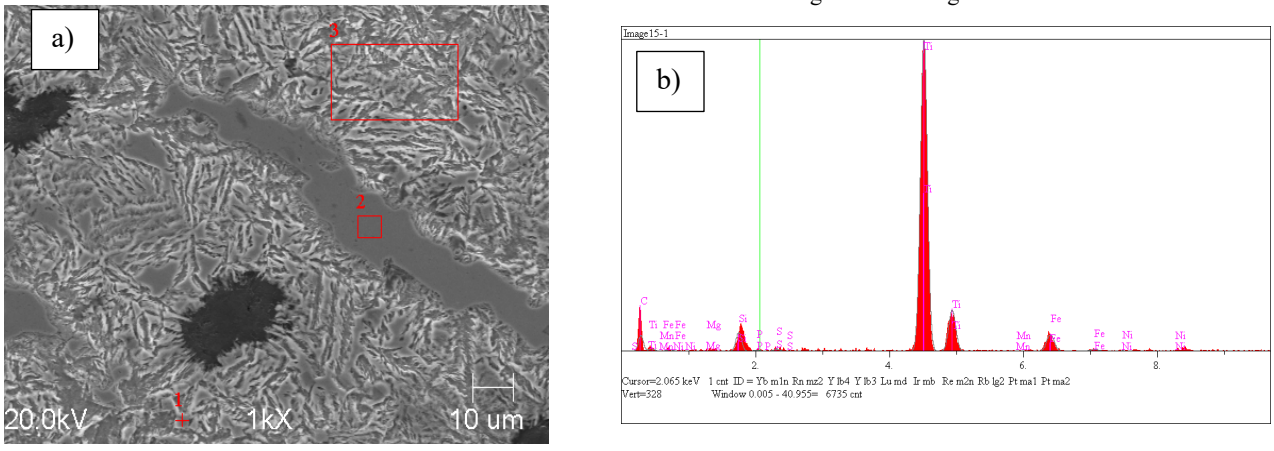

Fig. 5. SEM microstructure (a) and spectrum (b) for SGIb composite

Table 6.
EDS chemical composition results for SGIb composite

Spot	Chemical composition, % wt.								
	C	Si	Mn	P	S	Mg	Ni	Ti	Fe
1	*0.705*	*2.458*	*0.121*	*0.155*	*0.282*	*0.104*	*0.441*	*68.301*	*Bal.*
2	*2.404*	*0.262*	*0.052*	*0.105*	*0.029*	*0.220*	*0.764*	*0.176*	*Bal.*
3	*3.650*	*1.606*	*0.200*	*0.049*	*0.142*	*0.000*	*0.439*	*0.713*	*Bal.*

In the SGIb composite, an ausferritic matrix was obtained (figure 5), also in this case the proportion of cementitic eutectics was reduced, but not completely eliminated. The EDS spectrum (figure 5), together with the EDS chemical composition (table 6), confirms that the phases obtained and described are correctly identified. Also, as in previous cases, the presence of titanium in the matrix is noticeable. Also in this composite, blocky autenite precipitation is observed, analogous to that in the SGIa composite.

4. Conclusions

On the basis of the structural studies carried out and after analysing the results obtained, the following conclusions can be drawn:

1. Spheroidisation treatment resulted in a vermicular cast iron, as evidenced by an aspect ratio for graphite of 0.58.
2. The SHSB synthesis reaction initiated in the liquid melt resulted in a cast composite of MMCs types composed of titanium carbides up to 5 μm in size and an ausferritic metallic matrix.
3. Titanium carbides produced in the cast iron by the SHSB method crystallise in the form of faced crystals, with a volume share of about 4%.
4. None of the heat treatment variants carried out changed the morphology of the titanium carbides and their distribution in the melt volume, confirming the thermodynamic stability of these carbides.
5. The SHSB synthesis did not significantly affect the spheroidisation process, it is a completely separate process that does not affect other metallurgical steps, the only factor that affected the change in graphite morphology was the presence of titanium.
6. The composite of vermicular cast iron reinforced with titanium carbide particles after SHSB synthesis had a high proportion of cementitic eutectics in its structure, which was mostly eliminated by the proposed heat treatment (this applies to both variants).
7. The excessively high austenitisation temperature (temperature of around 900°C) resulted in the formation of blocky austenite in the microstructure in both heat treatment variants.

References

[1] Guzik, E. (2006). *Selected issues of forming the structure and properties of ausferritic cast iron.* Wydawnictwo Komisja Odlewnictwa PAN Katowice. (in Polish).

[2] Górny, M., Gondek, Ł., Tyrała, E., Angella, G. & Kawalec M. (2021). Structure homogeneity and thermal stability of austempered ductile iron. *Metalurgical and Materials Transactions A*. 52, 2227-2237. https://doi.org/10.1007/s11661-021-06214-8.

[3] Guzik, E. (2001). *Cast iron refining processes - selected issues.* Wydawnictwo Komisja Odlewnictwa PAN Katowice. (in Polish).

[4] Górny, M. (2017). Thin – wall gray iron castings. In D.Stefanescu (Eds.), *Cast Iron Science and Technology. Volume 1A* (pp. 575-582). ASM Handbook.

[5] Angella, G., Ripamonti, D. & Górny, M. (2020). Comparison between ductility examination and a new approch based on strain hardening analysis to support the determination of proper austempering times. *International Journal of Cast Metals Research*. 33(1), 50-60. https://doi.org/10.1080/13640461.2020.1746041.

[6] Opaliński, A. & Wilk–Kołodziejczyk, D. (2021). Information and decision system supporting the production of ADI cast iron products. *Archives of Metallurgy and Materials*. 66(2), 651-657. DOI: 10.24425/amm.2021.135903.

[7] Jakubus, A. (2022). Initial analysis of the surface layer of AVGI cast iron subject to abrasion. *Archives of Foundry Engineering*. 22(2), 50-56. DOI: 10.24425/afe.2022.140224.

[8] Tyrała, E., Górny, M., Kawalec, M., Muszyńska, A. & Lopez, H. (2019). Evaluation of volume fraction of austenite in austempering process of austempered ductile iron. *Metals*. 9(8), 893, 1-10. https://doi.org/10.3390/met9080893.

[9] Olejnik, E., Janas, A., Kolbus, A., Grabowska B. (2011). Composite layers fabricated by in situ technique in iron castings. *Kompozyty*. 11(2), 120-124.

[10] Szymański, Ł., Olejnik, E., Sobczak, J., Szala, M., Kurtyka, P., Tokarski, T. & Janas A. (2022). Dry sliding, slurry abrasion and cavitation erosion of composite layers reinforced by TiC fabricated in situ in cast steel and gray cast iron. *Journal of Materials Processing Technology*. 308, 117688, 1-15. https://doi.org/10.1016/j.jmatprotec.2022.117688.

[11] Fraś, E., Wierzbiński, S., Janas, A. & Lopez, H. (2001). SHSB processing and properties of Al/TiC "in situ" composites. *Archives of Metallurgy*. 46(4), 407-423.

[12] Merzanov, A. G., Styschev (2002). *Self-Propagating High-Temperature Synthesis of Materials* (vol.5). CRC Press.

[13] Szymański, Ł., Olejnik, E., Sobczak, J. & Tokarski, T. (2022). Improvement of TiC/Fe in situ composite layer formation on surface of Fe-based castings. *Materials Letters*. 309, 131399, 1-5. https://doi.org/10.1016/j.matlet.2021.131399.

[14] Kawalec, M. (2019). *Forming the structure of thin-walled castings made of high-quality cast iron with vermicular graphite precipitations.* Katowice: Wydawnictwo Komisja Odlewnictwa PAN. (in Polish).

[15] Stefanescu, D., Huff, R., Alonso, G., Larranga, P., De La Fuente, E. & Suarez, R. (2016). On the crystalization of compacted and chunky graphite from liquid multicomponent iron-carbon-silicon-based melt. *Metalurgical and Materials Transactions A*. 47, 4012-4023. https://doi.org/10.1007/s11661-016-3541-4.

[16] Zeng, D., Zhang, Y., Liu, J., He, H. & Hong, X. (2008). Characterization of titanium-containing compounds in gray iron. *Tsinghua Science and Technology*. 13(2), 127-131. https://doi.org/10.1016/S1007-0214(08)70022-1.